Evaluation of Pulmonary Systemic Blood Flow Using ECG Gated Acquisition

Joao J. Pedroso de Lima, Maria Filomena R. Botelho, Jose A.S. Rafael, Joao Bernardo, Lino M. Gonçalves, Maria de Fatima Pacheco, Cristina A. Santos, Antonio J. Pinto and Manuel D. Cerqueira

Biophysics Service, Faculty of Medicine, University of Coimbra; Department of Electronics and Telecommunications, University of Aveiro; Cardiology and Cardiothoracic Surgery Services, Hospital of the University of Coimbra, Coimbra, Portugal; and Department of Radiology, Division of Nuclear Medicine, University of Washington, Seattle, Washington

We propose a functional parametric analysis method using ECG-gated ^{99m}Tc-labeled red blood cell (RBC) imaging for detection and characterization of periodic variations in local blood activity in the lungs during cardiac cycle. We validated in animal experiments that such count variations correlate with cyclical pulmonary blood flow and may be used for evaluation of systemic-to-pulmonary shunts. Clinical studies were performed in 48 patients. After labeling the RBC pool with ^{99m}Tc, ECG-gated gamma camera images of both lung fields were acquired and processed to obtain Fourier transforms of time/activity functions in selected regions. The first harmonic parametric images of amplitude and phase were derived. There was an excellent correlation (r = 0.92) between activity variations and pulsatile flow measured by our method with that obtained by the thermodilution method in dog experiments (n = 10) after implantation of a systemic-to-pulmonary shunt. Patient studies showed the technique to be sensitive in detecting and quantifying abnormal systemic-to-pulmonary blood flow. Lung pulsatile flow can thus be noninvasively measured from functional parametric phase and amplitude images; the technique may be useful for detecting and quantifying abnormal systemic-to-pulmonary blood flow in man.

J Nucl Med 1993; 34:1441–1446

During the cardiac cycle there are cyclical variations in pulmonary pressure, blood flow and blood volume caused by the pulsatile nature of blood flow through the pulmonary circulation. These changes are observed in arteries, arterioles, capillaries and venules and are due to volume variations in compliant vessels as well as the opening and collapse of these vessels. Pulmonary capillaries are distensible. In the dog, about 13% of total lung compliance is capillary compliance (*1*). Volume variations in lung capillaries also correlate to arterial pressure variations (*2*). Pressure variations of about 12 mmHg in the pulmonary artery and 3–5 mmHg in the pulmonary capillaries have been observed; these changes in arterial pressure have been correlated with pulmonary blood volume but do not correlate with variations in venous pressure (*3*).

If the RBC pool is labelled with ^{99m}Tc, and if frame-mode, ECG-gated dynamic gamma camera image acquisition of the lung area is performed, local blood volume variations in the pulmonary circulation can be detected and measured on a pixel-by-pixel basis. Parametric functional amplitude and phase images similar to those derived for left ventricular evaluation can be generated to characterize pulmonary blood flow (*4–6*).

The purpose of our study was to validate this technique of lung functional parametric analysis in an experimental dog model using thermodilution measurements before and after placement of a systemic-to-pulmonary shunt. We also performed clinical studies in patients with known pulmonary circulatory abnormalities and compared the radionuclide measurements to other measurement techniques.

MATERIALS AND METHODS

Red Blood Cell Labeling

Both patient and animal studies were performed using *in vivo* labeling of the RBC pool. Following intravenous administration of stannous pyrophosphate, patients received 25 mCi (925 MBq) and dogs 10–15 mCi (370–550 MBq) of ^{99m}Tc-pertechnetate.

Image Acquisition

All studies were acquired on a GE400 AC gamma camera interfaced to a dedicated 5000/200 DEC Imaging System. Software acquisition and processing programs were developed and validated by our group (*7*). For human studies, posterior view, R-wave ECG-gated gamma camera images of the lungs were acquired for 20 min with the patients seated. All studies were acquired in frame mode using a 64×64 image matrix and 32 frames/R-R interval. The average framing interval was 25 msec and the total number of heart cycles per study ranged from 1200–2000. This resulted in variations of total counts per pixel, reflecting volume changes from 1100 to 1300 counts in the frame sequence collected during the cardiac cycle.

Patients were fully informed about the study and gave informed consent to participate. Animal studies were conducted in accordance with standards established at the University of Coimbra for care and performance of studies involving animals.

Received Jan. 2, 1992; revision accepted May 19, 1993.

For correspondence and reprints, contact J.J. Pedroso de Lima, Serv. de Biofisica, Fac de Medicina, 3049 Coimbra Codex, Portugal.

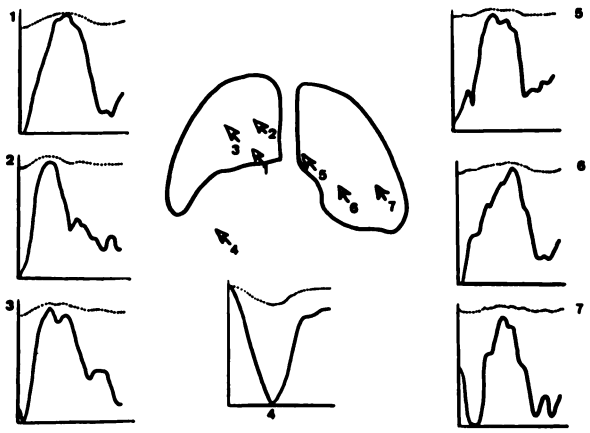

FIGURE 1. Schematic set of time/activity curves for 7 areas in the lung and left ventricle (area 4) of a normal control as seen in posterior view. Arrows indicate the sampling region. Dotted line curves are the actual measured count rates (y-axis) over time (x-axis). Solid line curves are normalized to maximum count variations.

Image Analysis

The summed-gated frames were reviewed visually and the lungs, heart and the great vessels manually defined by the operator. Regions of interest (ROI) were placed around the lungs in order to exclude the heart and great vessels. These regions generally excluded the mediastinal areas and the lower half of the left lung, which consists mainly of cardiac blood pool. ROIs were applied to individual frames to obtain time/activity curves on a pixel-by-pixel basis. Following Fourier transformation, the first harmonic amplitude and phase parametric images were created (*7*).

An example of this technique from a study performed on a normal volunteer is schematically shown in Figure 1. For each ROI, a cursor can be placed over a single pixel in the amplitude image and the absolute count rate as a function of time for this pixel and the adjacent 4 pixels is plotted. For each ROI, the absolute counts are plotted as dotted lines and the solid line curves have been normalized to the maximum observed variation. The 6 regions in the lungs (areas 1–3 and 5–6) achieve peak counts and the maximum count rate variation when counts are lowest in the left ventricular region (area 4). Regions near the hilum are fairly sinusoidal, but some deterioration in this function occurs toward the periphery (area 7).

Amplitude and phase images can be shown on the left of the display and histograms for number of pixels/phase angle are displayed to the right (Fig. 2). In addition, statistical parameters characterizing phase distribution for individual segments or total lung can also be derived.

Amplitude functional images are a measure of local variation of blood activity during the cardiac cycle and thus an indirect measure of pulsatile flow. Phase functional images show the instant of activity pulse in the lung pixels relative to the ECG R-wave gating signal. We found in healthy control patients an initial large peak corresponding to the pulmonary circulation and a second peak, with a greater phase angle and a smaller area, which corresponds to the pulmonary systemic blood flow. Because the phase origin in our lung phase histograms does not coincide with the ECG R-wave peak, we display our studies with a 270° shift to the right in the phase origin. This allows both the systemic and pulmonary peaks to be displayed without being sectioned by limits of the phase angle in the histogram. In subsequent discussions, phase angle values or timing during the cardiac cycle refer to the new, shifted origin.

The ratio of the sum of amplitudes of pixels in the phase interval of the systemic peak to the sum of amplitudes for all pixels in the lung ROI, regardless of phase, is called the amplitude ratio. The ratio is proportional to the fractional pulmonary-to-systemic flow ratio, which we validated in animal experiments.

Animal Experiments

Ten healthy mongrel dogs (6 females and 4 males) weighing 13.5 ± 5 kg (mean ± 1 standard deviation) were used. Following several days of observation, dogs were fasted for 12 hours and premedicated with IM ketamine (15 mg/kg), atropine (0.5 mg) and diazepam (5 mg) before anesthesia was induced with sodium pentobarbital (30 mg/kg I.V.). ECG electrodes were placed to allow gated acquisition; the dogs were positioned supine with limbs restrained. The thorax was opened by median sternotomy and the pericardium exposed. A pediatric 5F Swan-Ganz catheter was introduced through the right atrial appendage into the right atrium and advanced through the right ventricle into the pulmonary artery trunk. The catheter was stabilized when its terminal hole and the transducer were in the pulmonary artery and its proximal hole, used for the cardiac output injection, was in the right atrium. The blood pool of the dogs was radiolabeled and gated acquisition was carried out for 15 minutes. Cardiac output was measured by the thermodilution method using an Edwards Laboratories Cardiac Output Computer (model 9520A).

Next, a systemic-to-pulmonary shunt was created between the ascending portion of the aorta and the beginning of the pulmonary artery in each dog. Cardiac output measurements and ECG-gated blood pool acquisition were repeated. The difference between the flows in the pulmonary artery before and after the shunt implantation is the shunt flow which can be expressed as a fraction of the total flow in the pulmonary artery. Data from the first acquisition were processed using the method described above and the amplitude ratio for the bronchial circulation as a fraction of the total pulmonary flow was determined. From the second acquisition, the amplitude ratio for the flow corresponding to the implanted shunt plus the bronchial circulation was obtained.

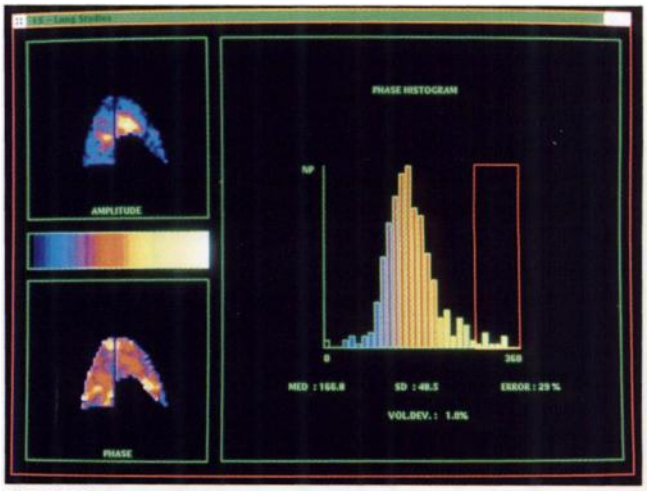

FIGURE 2. Amplitude and phase parametric images and phase histogram of a single representative dog before implantation of a systemic-to-pulmonary shunt.

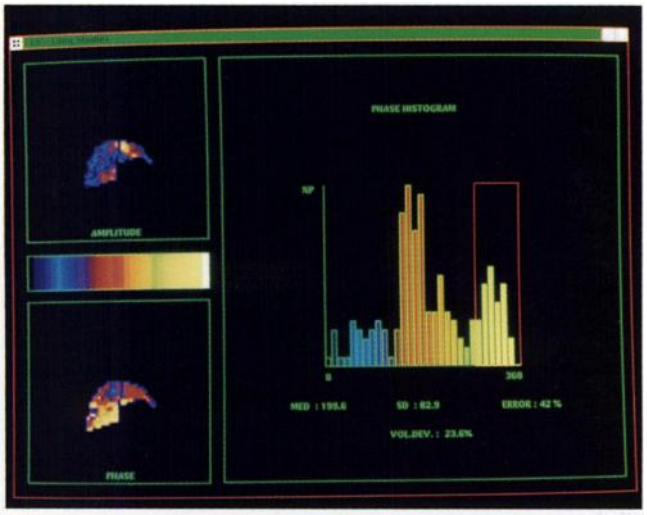

FIGURE 3. Amplitude and phase parametric images and phase histogram of same dog as in Figure 2 after creation of a systemic-to-pulmonary shunt. There was excellent correlation between the 2 methods (r = 0.918).

Patient Studies

Human studies were carried out in 48 patients: 25 controls, eight with chronic obstructive pulmonary diseases (COPD), 11 with systemic-to-pulmonary shunts, and four with pulmonary sequestra (a portion of lung supplied by a systemic artery arising from the aorta or one of its branches). The controls were volunteers whose blood pool was already labeled for clinically indicated ^{99m}Tc-radionuclide ventriculography and in whom absence of pulmonary disease had been confirmed.

Reproducibility

Since variability may occur in selecting ROIs, reproducibility of the technique was assessed. A total of 10 patient images were analyzed on two separate occasions by two observers with a minimum of 2 wk between processing.

Statistical Analysis

All values are shown as the mean ± 1 standard deviation. Agreement between the thermodilution flow ratio and the amplitude ratio measured from the functional images was performed using linear regression analysis. A $p < 0.05$ was considered statistically significant for all comparisons.

RESULTS

Animal Experiments

The average amplitude ratio for the area under the bronchial peak obtained in the dogs before the implant was 4.24 ± 2.56%. Figures 2 and 3 show the analysis before and after shunt implantation in a single dog. Table 1 compares the flow ratio obtained by the thermodilution technique to the amplitude ratio of shunt flow plus bronchial circulation obtained by the proposed radionuclide method in the 10 dogs. These results are plotted in Figure 4. There was excellent agreement between the two methods with r = 0.918 (p = 0.0002) and with the following regression equation:

$$\text{Amplitude Ratio} = 3.48 + 0.70 \times \text{FR}$$

TABLE 1
Flow ratio by the thermodilution method compared to the amplitude ratio for individual dogs.

Experiment number	Flow ratio by thermodilution (%)	Amplitude ratio radionuclide method (%)
1	4.0	5.8
2	10.0	12.8
3	15.8	10.1
4	11.9	11.6
5	5.5	4.8
6	4.3	10.1
7	30.0	23.6
8	22.2	21.1
9	16.6	17.4
10	6.6	6.0

The intercept of 3.48 suggests that our proposed method overestimates the thermodilution values. The standard error of the coefficient is 0.11 and the standard error is 1.60%.

Results in Humans

Representative examples of cases studied by this radionuclide method are presented in the following sections.

Control Cases. The amplitude functional image in a control case is shown at the upper left of Figure 5. It reflects the extent of activity (volume) variation of the pulmonary blood and, indirectly, pulsatile flow. The color scale indicates increasing values from blue (lowest) to white (highest). The yellow/red zones in the middle areas of the lungs are a result of strong pulsations in the large diameter arterial vessels of the hilum. At the lower left of Figure 5 is the phase functional image. Here the color scale refers to the 0–360° phase interval, matching the period of a sinusoidal function. Blue means small phase angles or short arrival times of pulsation in the pulmonary area.

The phase functional image shows that arrival times of blood volume wave are, on average, shorter in the left

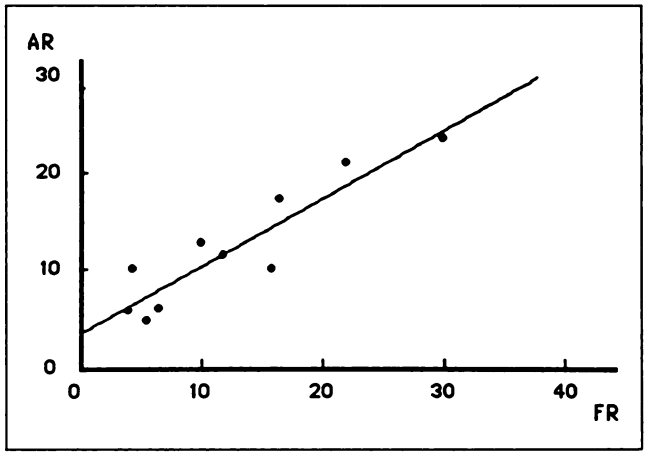

FIGURE 4. The amplitude ratio (AR) calculated by the radionuclide method is compared to the flow ratio (FR) measured by thermodilution for 10 dogs in which a systemic-to-pulmonary shunt was surgically created.

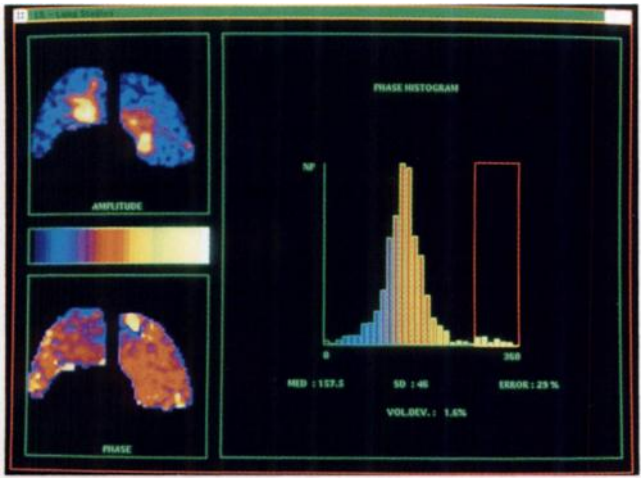

FIGURE 5. Amplitude and phase parametric images and phase histogram of a human normal control.

lung. Considerable homogeneity is observed for most of the lung in controls.

At the right hand side of Figure 5 is the phase histogram for the total lung area. The phase angle mean value, standard deviation and its percent value with respect to the mean can also be seen. The pixel color scale used in the phase functional image as described above is maintained in this histogram.

The phase histogram shows that pulsation arrival time in the pulmonary area has a small spread with respect to the mean. Taking into account all the pixels in the ROI, the value was 157.5 ± 46° (mean ± SD).

Abnormal Studies

Two pathological clinical cases studied with the present method are presented in Figures 6–10.

Case 1. Figure 6 presents the results of a patient with pulmonary sequestrum at the base of the right lung confirmed by aortography. The amplitude parametric image shows an area of medium amplitude in the left lung that

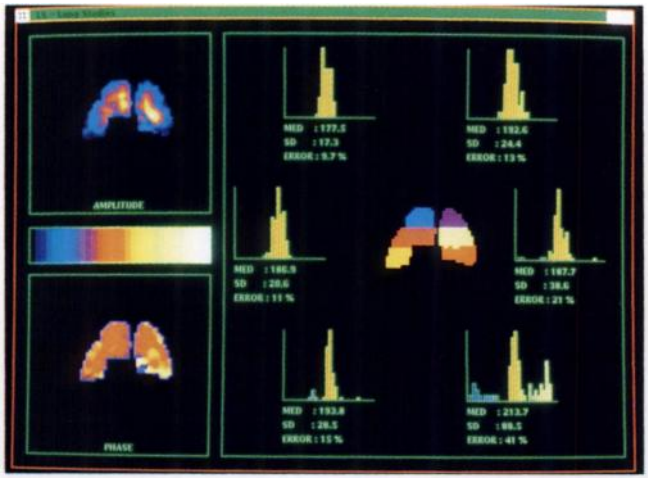

FIGURE 6. Amplitude and phase parametric images (left panels) and phase histograms for apex, middle and basal thirds of each lung in a patient with a pulmonary sequestrum at the base of the right lung. An area with large phase angle is observed at the base of the right lung.

FIGURE 7. Anterior abdominal aortography of patient in Figure 6. An abnormal branch of the celiac axis heads to base of right lung (arrow) and is consistent with pulmonary sequestra.

starts in the medial hilar region and extends to the periphery. In the right lung, the hilar area of high amplitude extends down obliquely to the base. The phase image shows abnormally long arrival times at the base of the right lung. The phase histogram of the lower third of the right lung shows a peak phase near 360°. The pixels in the phase functional image contained in this peak have the same color as in the histogram and they correspond to the sequestrum region. The percent amplitude ratio for the small peak (yellow-to-white) is 3%. These findings were confirmed by aortography which showed an abnormal branch of the celiac axis heading to the base of the right lung (Fig. 7).

Case 2. The study from a patient with a systemic-to-pulmonary shunt in the left lingula, confirmed by pulmonary arteriography, is shown in Figure 8. In the amplitude functional image, high amplitude areas similar to large vessels and running downward from the hilar regions, are observed in both lungs. At the lung periphery, the amplitudes are very small or virtually absent. The phase functional image indicates that the high amplitude areas have a large phase angle. Outside these areas the phase distribution is close to normal.

Points ranging from yellow to white inside the window in the phase histogram for the total pulmonary ROI, and pixels with the same colors in the phase functional image in

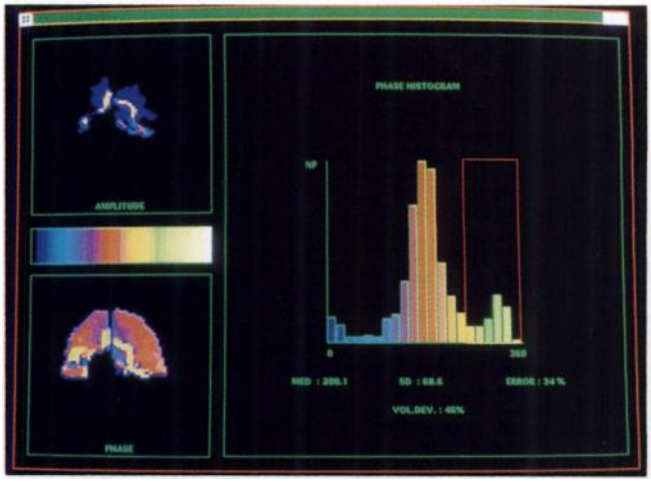

FIGURE 8. Functional parametric images in patient with systemic-to-pulmonary shunt. Areas of high amplitude value and large phase angle observed in both lungs.

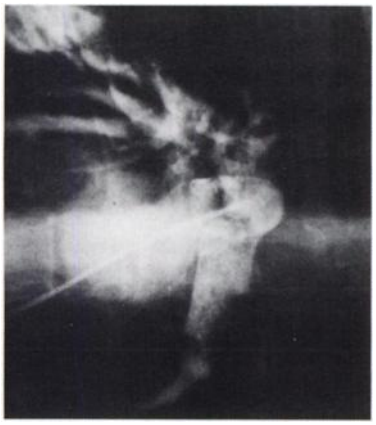

FIGURE 9. Pulmonary angiography of patient in Figure 8.

Figure 8, are due mainly to late arrival in the lungs of blood from the shunt. The calculated amplitude ratio was 46%. The pulmonary arteriogram for this patient is shown in Figure 9. After surgical resection of the lingula, the radionuclide study was repeated and the results shown in Figure 10. The pathological findings on the surgical specimen described arteriovenous lesions with fibromuscular thickening of arterioles associated with luminal reduction, venular dilatation and angiodysplasia.

Table 2 shows mean results of percent amplitude ratio values for pixels of phase angle above the pulmonary circulation peak, for all 48 patients studied. There were 25 controls with very small mean ratios and a small variability as shown by the small standard deviation of 1.6%. Eleven patients with systemic-pulmonary shunts had the largest amplitude ratio values. Seven patients with chronic obstructive pulmonary disease and four with pulmonary sequestra also were studied and the radionuclide derived amplitude ratios were all abnormal.

Angiography was performed in 19 of cases studied (four with chronic obstructive pulmonary disease, 11 systemic-to-pulmonary shunts and four pulmonary sequestra). A comparison between radiographic data and noninvasive radionuclide method results showed a good relationship between derived amplitude ratio values and anatomic findings.

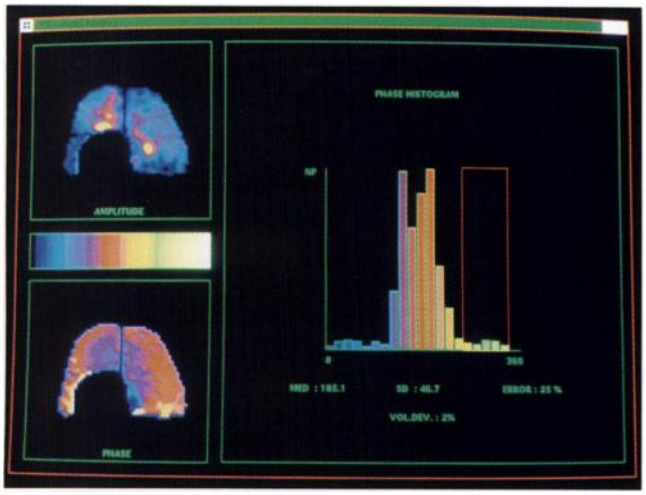

FIGURE 10. Functional parametric images of patient in Figure 8 after surgery.

TABLE 2
Radionuclide derived amplitude ratios in 25 controls and 23 patients with various types of lung disease.

	N	%
Controls	25	1.9 ± 1.6
COPD	8	7.4 ± 3.0
S-P Shunts	11	15.7 ± 5.4
Pulmonary Sequestra	4	3.2 ± 0.6

COPD = chronic obstructive pulmonary disease
S-P = systemic-to-pulmonary shunt

Reproducibility

There were no significant interobserver or intraobserver differences for calculated amplitude ratios using the entire lung fields.

DISCUSSION

Results from our animal validation study showed good correlation between amplitude ratio calculated by the proposed radionuclide method and flow ratio measured by the thermodilution method. In calculating the amplitude ratio values, the bronchial circulation is added to shunt flow. In Figure 4, the intercept of the regression line through the amplitude ratio axis should then be related to the bronchial flow. The intercept is 3.46% (standard error—1.60%), which is close to the average value of the amplitude ratio obtained before the shunt implantation (4.24 ± 2.56%). This explains the systematic overestimation.

Information contained in parametric images of amplitude and phase is clinically important. The first harmonic amplitude parametric images, although indicating local pulsation, do not have the same information as the classical ^{99m}Tc-MAA perfusion images routinely obtained. The latter technique visualizes the vascular tree that retains the radioactive particles, i.e., mainly arterioles and capillaries. In our functional radionuclide ECG-gated method, vascular territories are visualized in which considerable variations of blood volume (or blood activity) occur during the cardiac cycle, i.e., the great pulmonary arteries, the arterioles and, to a lesser extent, the pulmonary capillary network. These are the vessels at which clinically significant shunts or vascular abnormalities need to be detected.

In the lung circulation, the greatest volume variations normally take place in the great arterial vessels and these have the greatest amplitudes in the amplitude image. Visualization of these larger diameter vessels is not possible using ^{99m}Tc-MAA perfusion images. One limitation of our method is the exclusion of the hilar area of the left lung, which is superimposed over the heart and aorta. This makes it difficult to analyze this portion of the left lung amplitude images and make comparisons between the proximal arterial portions of both lungs.

The first harmonic phase functional image and phase histogram are important in characterizing timing of blood volume changes and flow waves. In control patients, with

the areas of heart and aorta excluded from the lung ROI, the phase histogram shows a large peak (pulmonary circulation peak) followed by a very small peak (bronchial circulation peak), which sometimes is not easily detected, as illustrated in Figure 5. However, if pulmonary ROI is allowed to include large vessels above the heart, a new peak with a phase angle similar to that of the bronchial peak is observed. If the same procedure is carried out in patients with systemic-to-pulmonary shunts, the great vessels and shunt peaks, in the phase histogram, are virtually superimposed.

We compared results by the proposed radionuclide functional image method with results by angiography in 19 of the cases in which vascular alterations of pulmonary circulation were confirmed. There was good agreement between the two methods, and the radionuclide method provided not only visualization of abnormalities, but also quantification of flows. The existence of an enlarged "systemic" peak in phase histograms in cases of proven increases of systemic flow and visualization of shunts in phase images with the same localization as in the arteriograms was observed.

An inherent error associated with the first harmonic amplitude and phase images is the "a priori" assumption that time/activity functions for the pixels are sinusoidal functions. This assumption may vary from patient to patient and also with patient position. The normalized time/activity curves obtained from points on the lung ROI indicate in most cases studied that errors resulting from this approximation may be small, particularly in healthy controls (Fig. 1).

If a perfect fit to a sinus function is assumed, error of the amplitude of the first harmonic, in the present method, is less than 15% in healthy controls (see Appendix). Error associated with evaluation of the amplitude ratio, calculated as a ratio of the summations of the pixel amplitudes in phase intervals of the shunt and of the total histogram, is not easy to obtain for humans. The value of 1.9 ± 1.6 was obtained as the normal amplitude ratio for the systemic blood flow arriving at the pulmonary area, with phase greater than the peak of pulmonary circulation (*8*).

One possible situation in which quantitative information can not be obtained by this method is when phases of the pulmonary and systemic flows cannot be separated in the histogram. This occurred in two patients with mixed pathology. The sensitivity of the method has also been verified in several situations in which small systemic-to-pulonary flows, barely detectable by angiography were detected by the phase images. Further work is required.

CONCLUSIONS

The present work demonstrates the ability to acquire dynamic information about lung pulsatile flow noninvasively in order to detect and quantify systemic-to-pulmonary flows noninvasively. Animal experiments demonstrated an excellent correlation between activity pulsation and pulsatile blood flow and showed that, under experimental conditions, amplitude ratio calculated by this method correlated well with flow ratio measured by thermodilution in the relative evaluation of flows in systemic-to-pulmonary shunts.

Results obtained in patients demonstrated the technique to be easily obtained, valuable, and complementary. Absent other noninvasive techniques to obtain these data, the proposed radionuclide method of functional parametric analysis could have a role in characterizing pulmonary circulation.

APPENDIX

In each of the 32 posterior-view ECG-gated frames (64×64) acquired over 1500 cardiac cycles, the average number of counts per pixel is about 1200. About 10% variation is observed in the time/activity curve for the pixels. If A1 = 1260 for the maximum value and A2 = 1140 for the mean, and assuming a sinusoidal variation, the relative standard deviation of amplitude of the first harmonic of the Fourier series is approximately (*4*):

$$\sigma_r = \frac{\sigma_h}{H} = k\sqrt{\frac{2}{n\bar{A}}}$$

Where $\bar{A}$ is the average number of counts in the pixel through the cardiac cycle, k is the ratio between $\bar{A}$ and the amplitude, H of the first harmonic and n the number of frames. For values of A1 and A2 taken before, n = 32 and k = 20, the relative standard deviation of the amplitude of the first harmonic is 0.14.

ACKNOWLEDGMENTS

The authors thank Prof Dr A.J.A. Robalo Cordeiro, Head, Center of Pulmonary, University of Coimbra, and his staff, Prof Dr L. Providencia, Head, Service of Cardiology, Hospital of the University of Coimbra, for the facilities made available to implement this work. The authors are also indebted to Laboratorio Nacional de Engenharia e Tecnologia Industrial (LNETI, CDI-U 068/86) and the International Atomic Energy Agency (IAEA, R.C. n 25123/R/RB) for financial grant support.

REFERENCES

1. Green JF. Mechanical concepts in cardiovascular and pulmonary physiology. Lea and Febiger: Philadelphia 1977;27–29.
2. Fung YCB, Sobin SS. Mechanics of pulmonary circulation. In: Hwang and Norman, eds. *Cardiovascular dynamics and measurements*. New York: University Park Press; 1977;667–675.
3. Caro CG, Pedley TJ, Schroter RC, Seed WA. *The mechanics of the circulation*. Oxford: Oxford University Press; 1978;493–508.
4. Frais MA, Botvinick EH, Shosa DW, et al. Phase image characterization of ventricular contraction in left and right bundle branch block. *Am J Cardiol* 1982;50:95–105.
5. Botvinick E, Frais M, O'Connell W, et al. Phase image evaluation of patients with ventricular pre-excitation syndromes. *J Am Coll Cardiol* 1984; 3:799–814.
6. Dae MW, Botvinick EH. Characterization of conduction and concentration abnormalities by scintigraphic phase analysis. *Int J Cardiol* 1984;5:244–53.
7. de Lima JJP, Rafael JAS and Botelho MFR. Dynamic imaging of the compliant perfusion of the lungs. *Eur J Nucl Med* 1986;12:258–262.
8. Bruner HD, Schmidt CF. Blood flow in the bronchial artery of the anesthetized dog. *Amer J Physiol* 1947;148:648. /Cit. in Harris P, Heath D. *The human pulmonary circulation*. 3rd ed, Edinburgh: Churchill Livingston: 1986;605–611.